

# Quantum transport and nanoplasmonics with carbon nanorings - using HPC in computational nanoscience

M. Jack<sup>1</sup>, A. Byrd<sup>1</sup>, L. Durivage<sup>2</sup>, and M. Encinosa<sup>1</sup>

Florida A&M University, Physics Department, FL<sup>1</sup>

Winona State University, Physics Department, MN<sup>2</sup>

78th Annual Meeting of the Southeastern Section of the APS

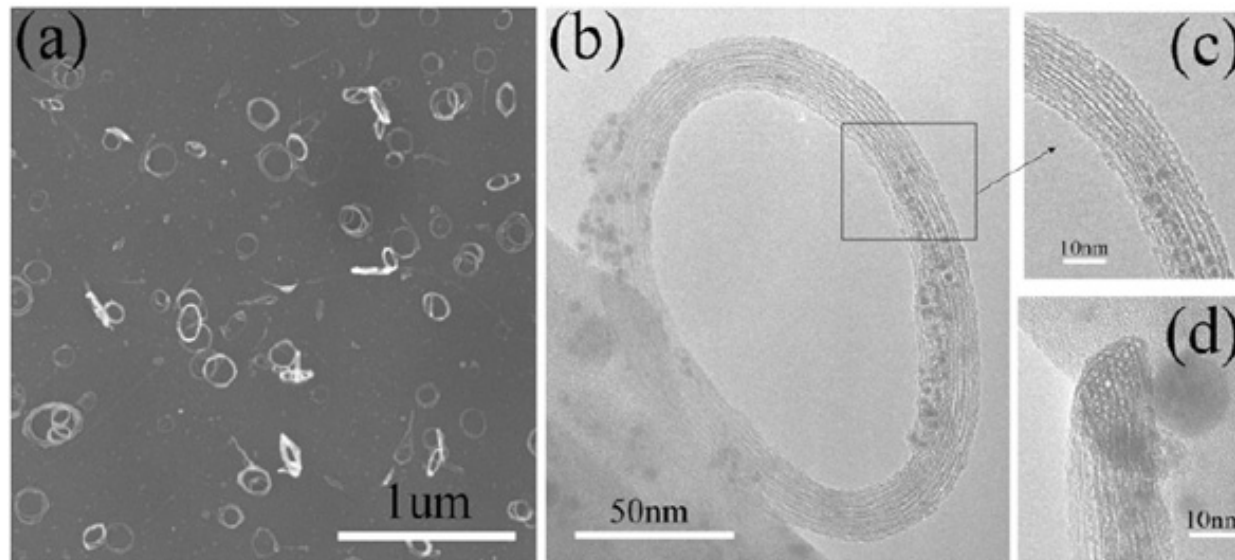
October 19-22, 2011

The Hotel Roanoke and Conference Center, Roanoke, VA

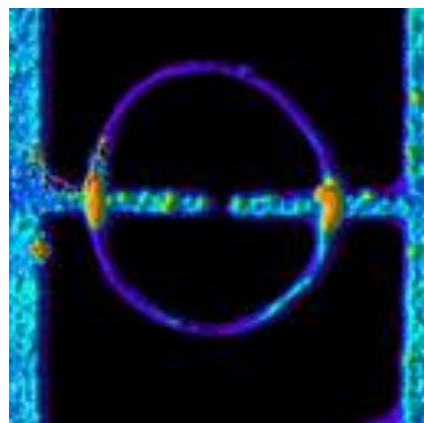




## Toroidal carbon nanotubes



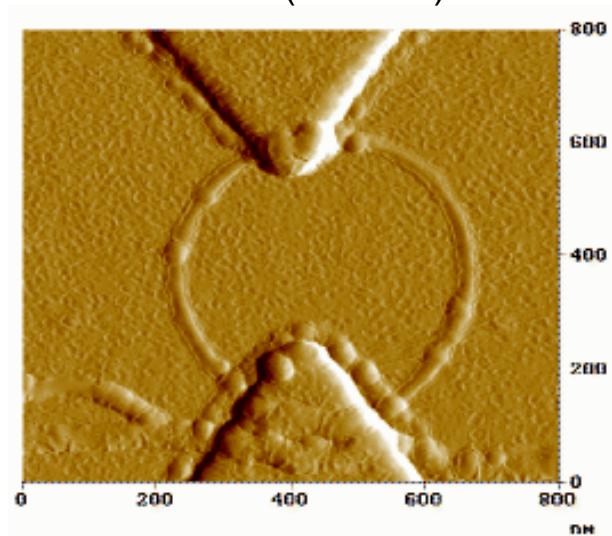
P. Avouris (IBM):



*Discovery:*

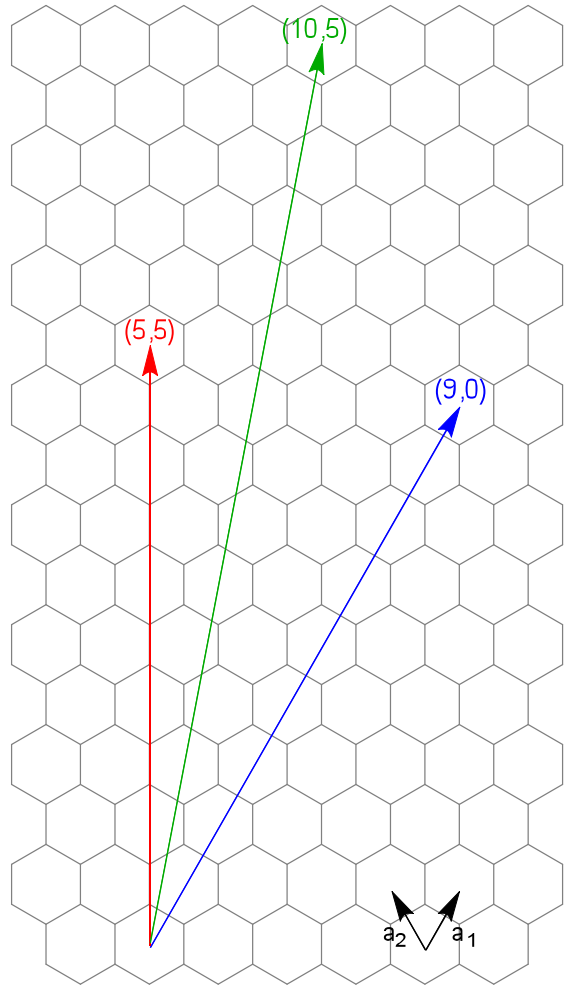
*S. Iijima, Nature 56  
(1991).*

C. Dekker (TU Delft):





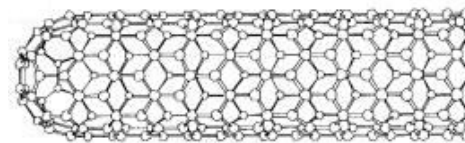
# Nanotube Structure



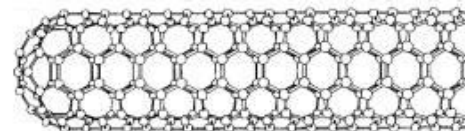
Iijima, *Nature* 363 (1993)  
Odom et al., *Nature* 391 (1998)  
Dai, *Acc. Chem. Res.* 35 (2002)

$(m,n)$  lattice vector:

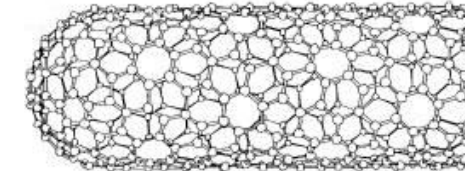
$$\mathbf{v} = m\mathbf{a}_1 + n\mathbf{a}_2$$



Zigzag (9,0)



Armchair (5,5)



Chiral (10,5)

# Metamaterials – carbon nanoring arrays and plasmonics



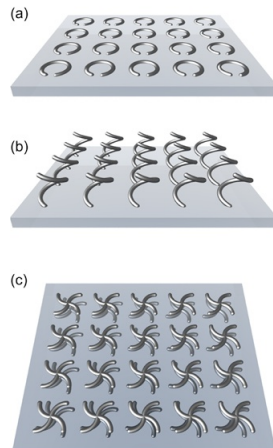
2010

NSF TeraGrid Pathways Program



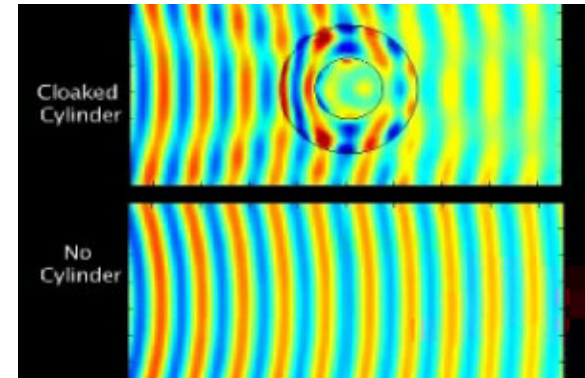
Idea:

- ✧ Create regular 2-dim lattice of carbon nanorings (armchair, zigzag, chiral).
- ✧ Drive electrical currents with external (coherent) light source.
- ✧ Electromagnetic multipole interference generated from array of ring currents.  
=> *Optical activity*: negative refractive index, dichroism, birefringence etc.



*Lattices of  
'chiral molecules'*

Schurig et al., Science 314, 977 (2006)

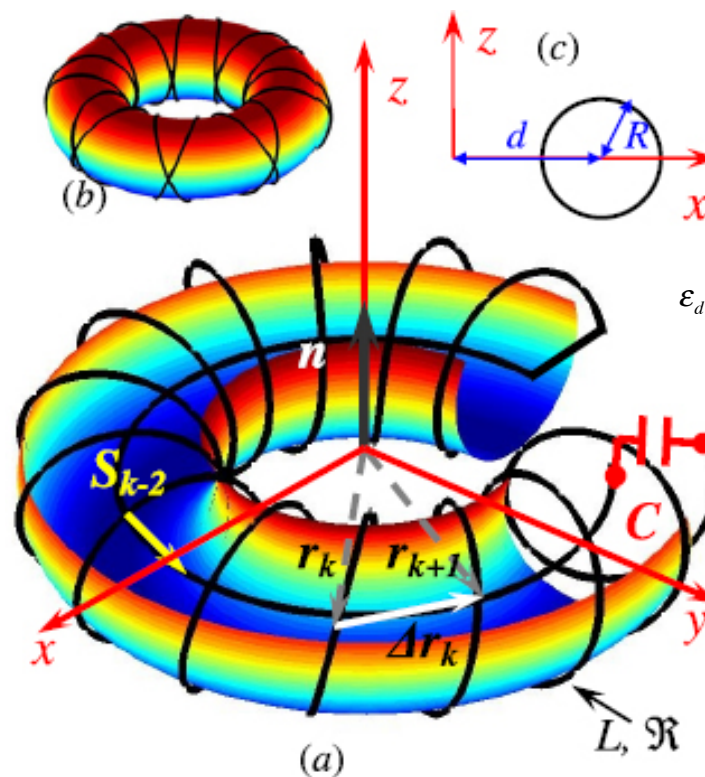


*Wegener  
and Linden,  
Physics 2, 3 (2009)*

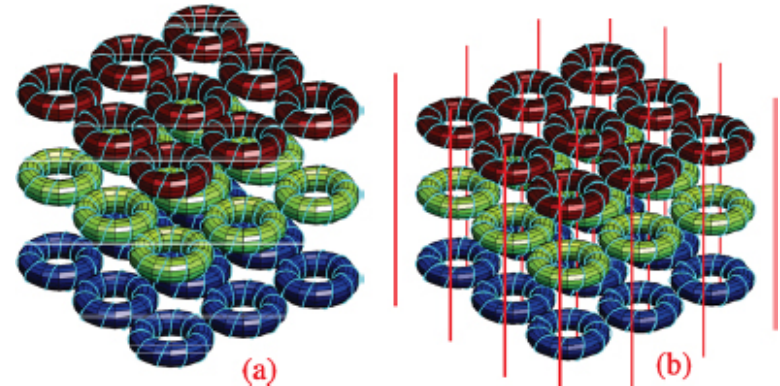
## Classical Theory – microscopic model for toroidal moment



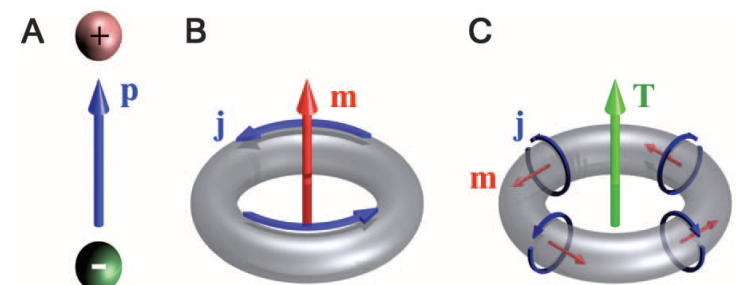
*Toroidal moment generated by microscopic ring currents:*



**K. Marinov et al., New J. Phys. 9 (2007):** a) Singly wound toroid with extra loop (no magn. dipole mom.); b) doubly wound toroid (no magn. di-/quadrupole mom.).



3D array of toroidal solenoids in a medium → *optical activity*



**Kaelberer et al, Science 330 (2010):** Toroidal moment  $\mathbf{T}$  generated by poloidal currents.



## ***Metamaterials for new energy applications***

- ✧ ***Metamaterials –***

Design of new optically active materials from the nanoscale up.

- ✧ Design a metamaterial with high energy storage density capabilities (new thin-film batteries) or with increased photoabsorption in organic photovoltaics (new thin-film solar cells).

- ✧ Benefit from synergy of:

- ✓ quantum coherence in nanoscale charge transport;
- ✓ unique optical response characteristics of chiral nanoconstituents;
- ✓ macroscopic interference for electromagn. energy storage and transport.

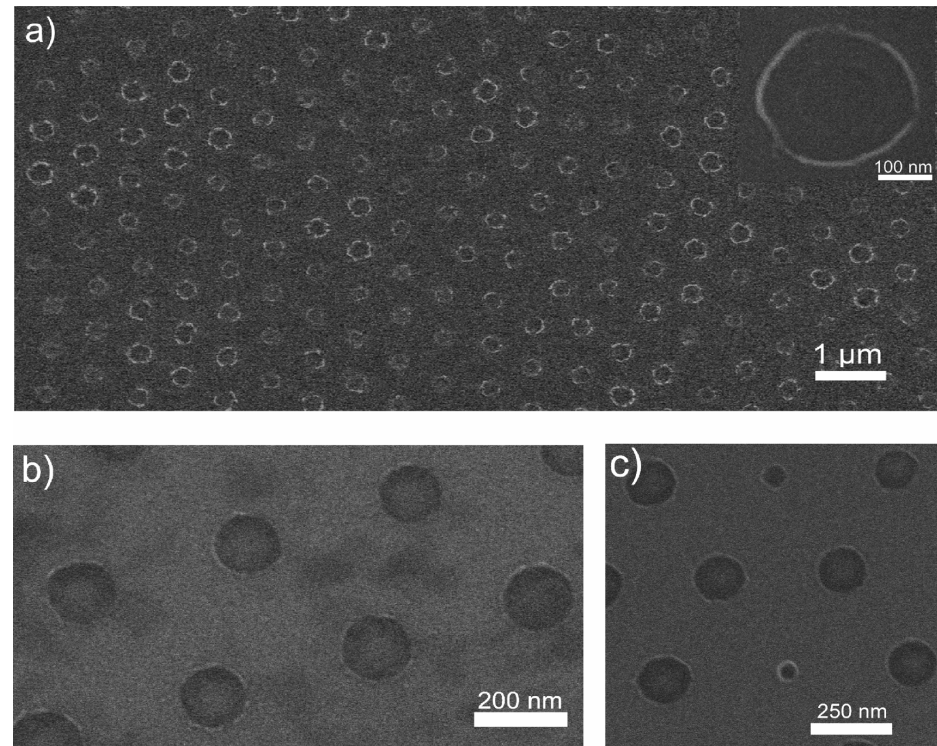
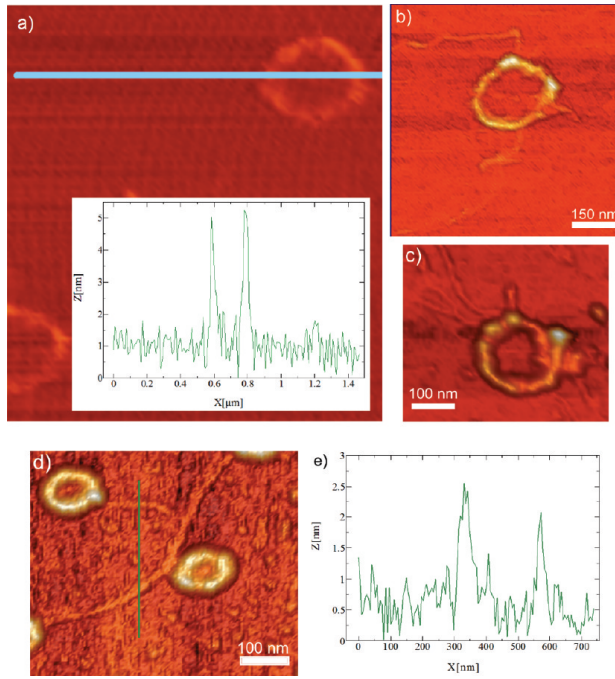
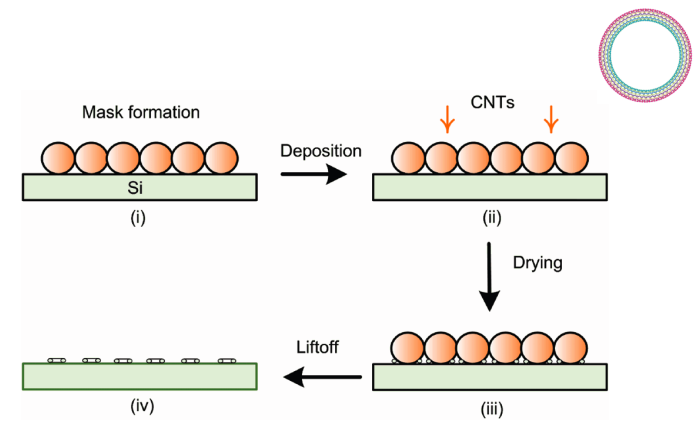
- ✧ Possibility of integrating photovoltaic energy generation and storage at the device level.

**Metamaterial with *array of carbon nanorings*  
with unique optical activity due to *nanoplasmonics*.**

➔ *Theoretical study from the quantum to the materials level.* 6

## **Ring synthesis and pattern formation:**

*Motavas, Omrane, and Papadopoulos:  
Large-Area Patterning of Carbon Nanotube  
Ring Arrays,  
Langmuir 2009, 25(8), 4655–4658.*





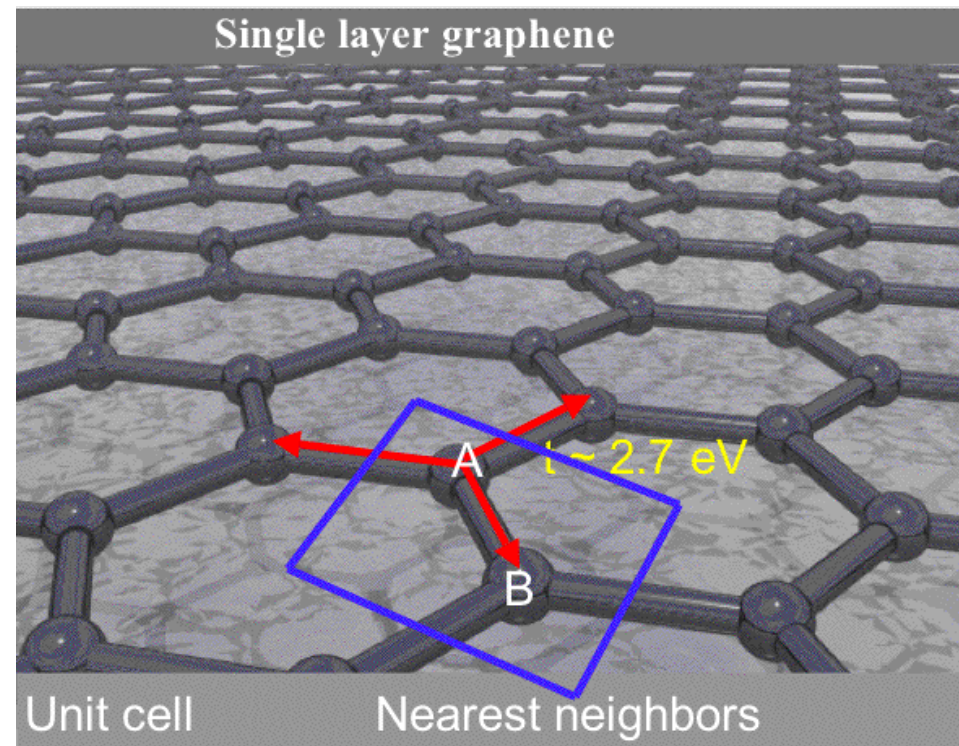
# Quantum Field Theory: Non-Equilibrium Green's Function Method (NEGF)

Hamiltonian  $H$  for electron transport in *tight-binding approximation*:

$$H = \sum_i E_i c_i^\dagger c_i + \sum_{i>j} (t_{ij} c_i^\dagger c_j + h.c.) \quad \text{ballistic transport}$$

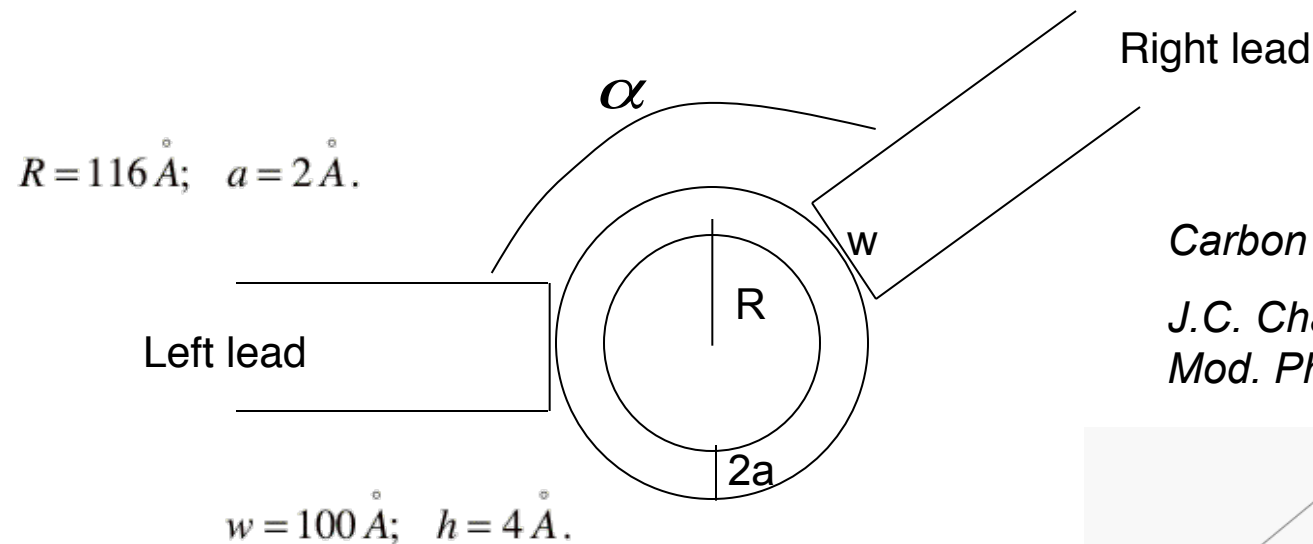
Example for  
tightbinding scheme:  
Single layer graphene

Graphene review:  
A.H. Castro Neto et al.,  
Rev. Mod. Phys. 81,  
109 (2009).

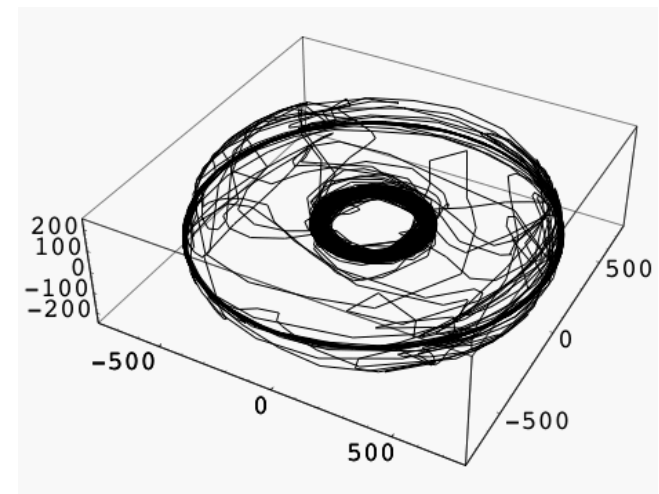
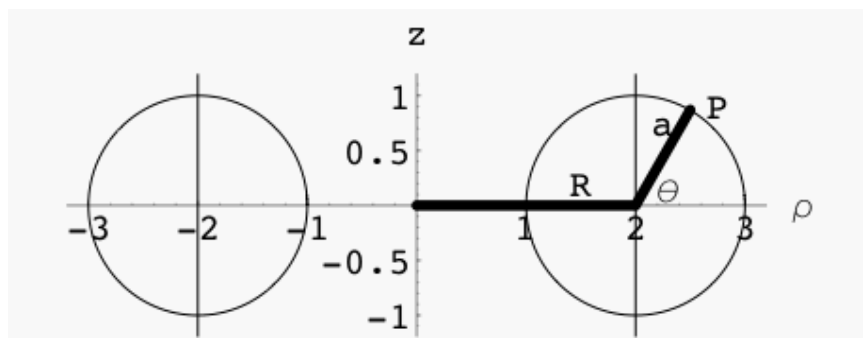




## Currents in a single nanoring – nanodevice model



*Carbon nanotube review:*  
J.C. Charlier et al., Rev.  
Mod. Phys. 79 (2009).



$$\bar{r}(\theta, \varphi) = (R + a \cos \theta) \hat{e}_\rho + a \sin \theta \hat{e}_z$$

Nanotorus with semi-infinite metallic leads. (3,3) armchair torus.



## Recursive Green's Function Algorithm (RGF)

Example: Green's function  $G_d$  for transport in a nanoring device:

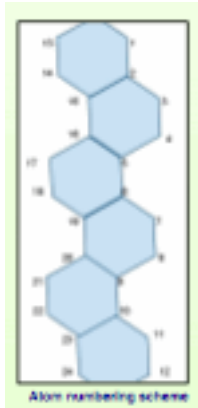
$$H'G_d = [E - H - \Sigma_L - \Sigma_R \pm i\eta]G_d = I$$

Effective Hamiltonian  $H'$ :

$$H' = \begin{pmatrix} A_1 & -V^\dagger & 0 & \dots & 0 & U^\dagger \\ -V & A_2 & -V^\dagger & \ddots & 0 & 0 \\ 0 & -V & \ddots & \ddots & \ddots & \vdots \\ \vdots & \ddots & \ddots & \ddots & \ddots & 0 \\ 0 & 0 & \ddots & \ddots & \ddots & -V^\dagger \\ U & 0 & \dots & 0 & -V & A_n \end{pmatrix}; \quad \begin{aligned} U &= -V \\ (A_i, U, V) &: 12 \times 12 \end{aligned}$$

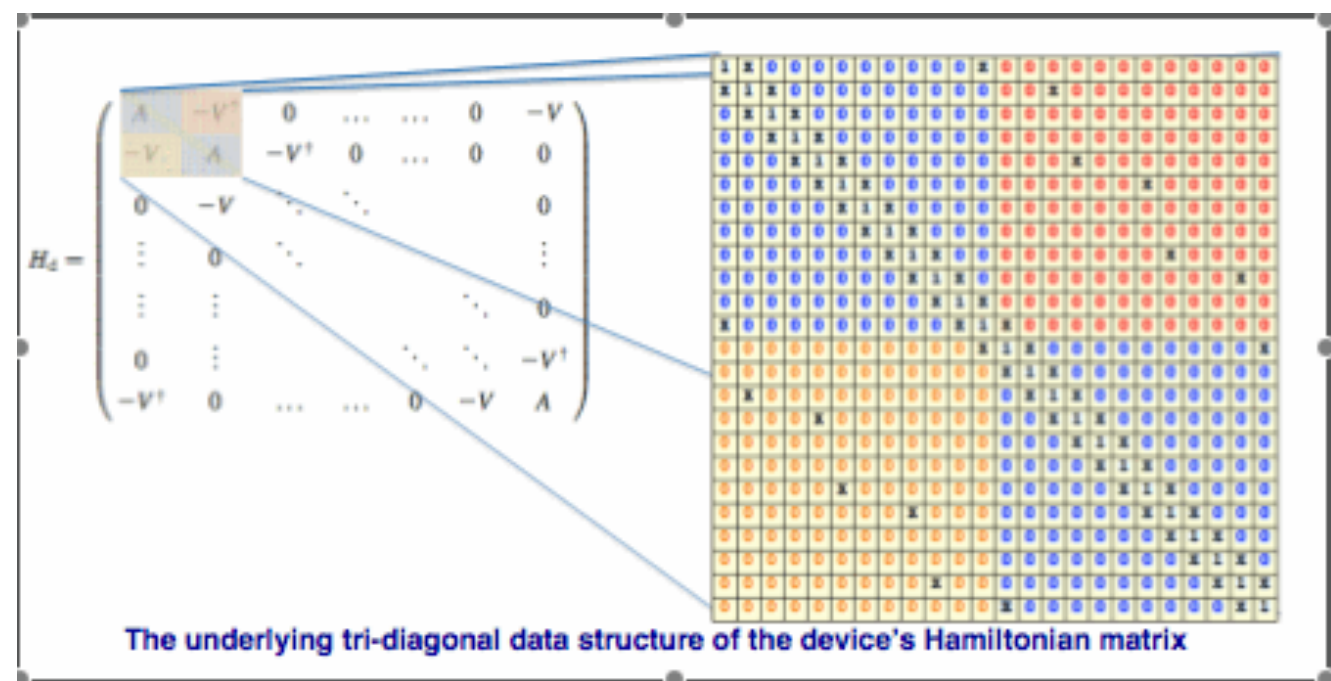
(3,3) armchair nanotorus

## Algorithm



The C atoms can be numbered in consecutive rings in the rolled-up graphene sheet.

Including only nearest-neighbor interactions the Hamiltonian matrix has the (mostly) *tridiagonal* structure shown at the right.



2010 TeraGrid Pathways Project with summer student [Leon Durivage \(Winona State U.\)](#) and [2010 NCSI/Shodor Blue Waters Undergraduate Petascale Computing and Education Program \(UPEP\)](#).



## **Density-of-states and transport observables**

Local density-of-states  $D(E)$ :

$$D(E) = G_d (\Gamma_L + \Gamma_R) G_d^\dagger$$

Transmission function  $T(E)$ :

$$T(E) = \text{Trace} [\Gamma_L G_d \Gamma_R G_d^\dagger]$$

Source-drain current  $I$  (Landauer-Büttiker):

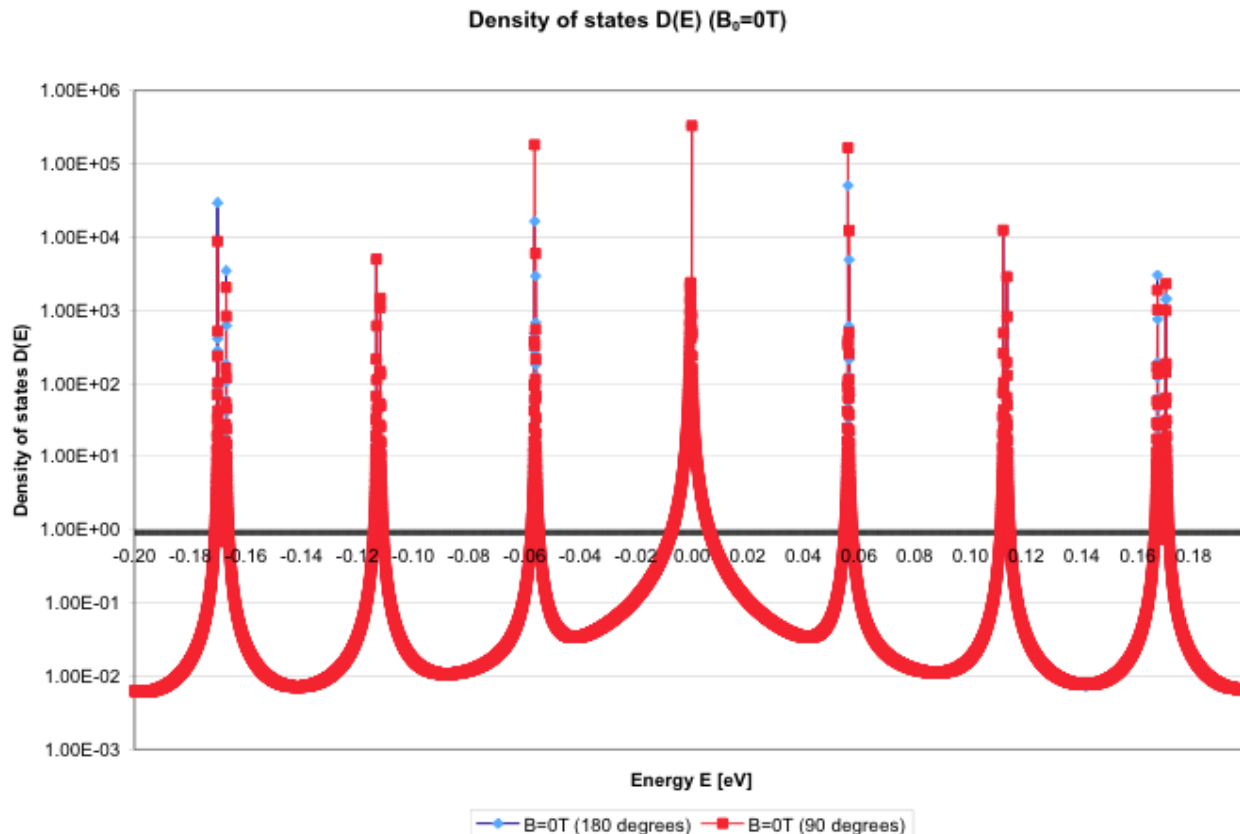
$$I = \frac{2e}{\hbar} \int_{-\infty}^{\infty} dE T(E) [f_0(E - \mu_1) - f_0(E - \mu_2)]$$



## Density-of-states $D(E)$

Compare different lead angles:  $\alpha = 90^\circ$  and  $\alpha = 180^\circ$  ( $B = 0$ ).

**N = 3600 atoms**

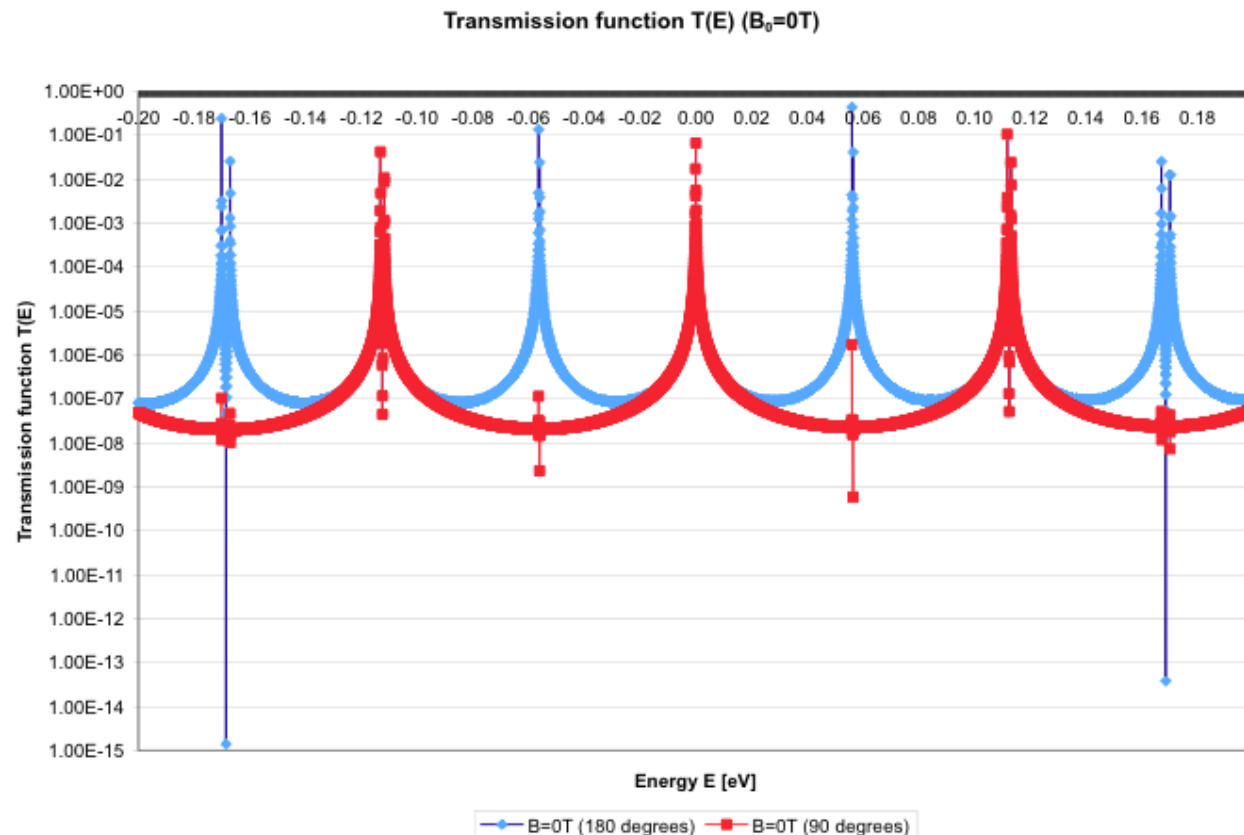




## Transmission function $T(E)$

Compare different lead angles:  $\alpha = 90^\circ$  and  $\alpha = 180^\circ$  ( $B = 0$ ).

**N = 3600 atoms**



Comparison: Magnitude of  $T(E)$  scales to that of 2-dim graphene ring.

*P. Recher et al., PRB 76, 235404 (2007).*



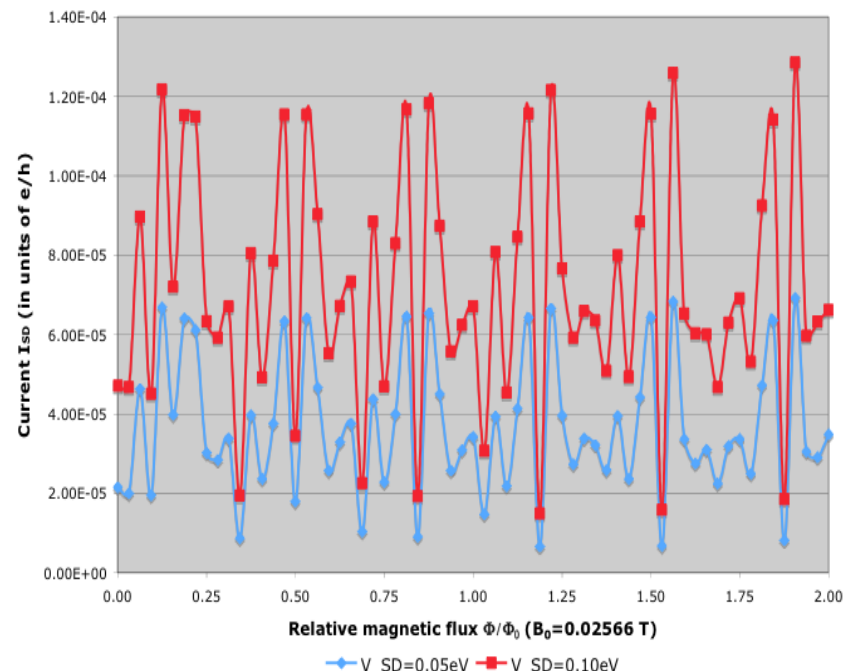
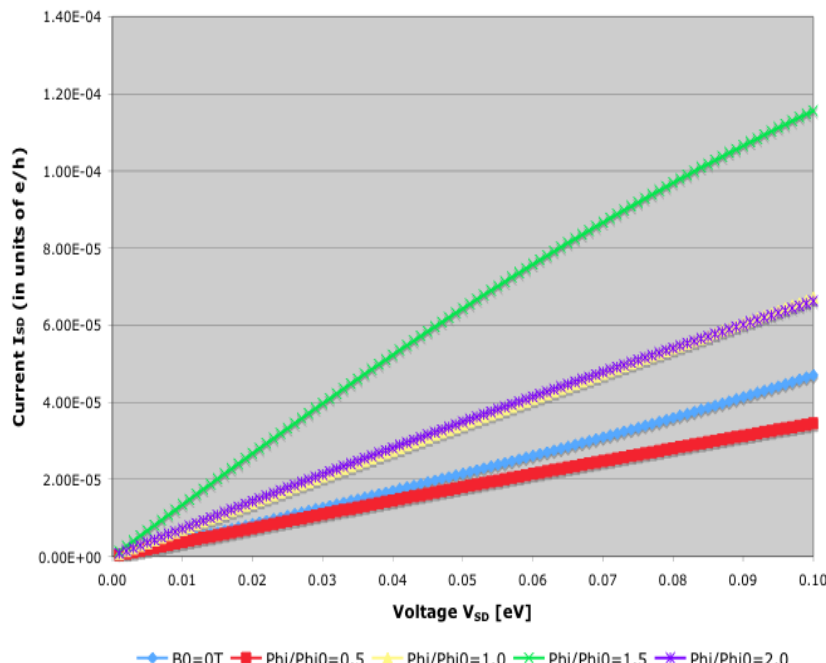
# Magnetic flux oscillations

## 90° angle between leads

a. Source-drain current  $I_{SD}$  as a function of source-drain voltage  $V_{SD}$  [eV] (small bias) for different magnetic fields  $B_0$ .  $I_{SD}$  in units of  $e/h$ .

Chemical potential at left/right lead:  $\mu_{1,2} = +/- V_{SD}/2$ . Thermal energy:  $k_B T = 30 \text{ meV}$ .

b. Source-drain current  $I_{SD}$  as a function of applied magnetic field  $B_0$  [T] ( $eV_{SD} = 0.05\text{eV}, 0.1\text{eV}$ ).



Torus size: N=1800 atoms



## Symmetries between armchair and zigzag tori – transport and band structure

Torus parameterization  $(m,n,p,q)$  –

Radius, chirality, length and twist of underlying  $(m,n)$  nanotube.

→ Physically distinct  $(m,n,p,q)$  armchair, zigzag and chiral tori  
with identical spectral and transport properties.

↔ Modular symmetries  $S, T$ :

$$S : \begin{cases} m \rightarrow -p \\ n \rightarrow -q \\ p \rightarrow m \\ q \rightarrow n \end{cases} \quad T : \begin{cases} m \rightarrow m \\ n \rightarrow n \\ p \rightarrow p+m \\ q \rightarrow q+n \end{cases}$$

Geometric symmetries  
due to compactification of  
2-dim graphene sheet  
to a torus surface  
**(NOT translational  
or rotational** symmetries  
of graphene lattice).

→ dramatic reduction of *spectrally distinct* nanotori classes, also  
with enclosed magnetic flux  $\Phi$ .



## Symmetries between armchair and zigzag tori – transport and band structure

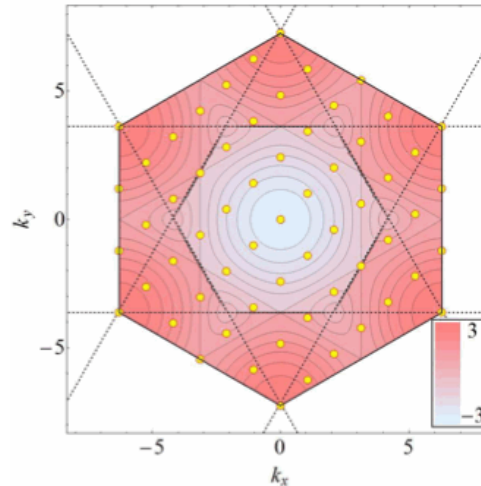
Examples:

*Identical energy spectrum for chiral tori*  
 $(3,2,24,10)$ ,  $(7,3,-22,-12)$ ,  $(8,6,-25,-21)$

12,205 physically distinct  
 nanotori ( $m,n,p,q$ )  
 $(N_{\text{hex}}=18, \Lambda=100, L_2 > 3L_1)$

→ 4 of 14 spectrally distinct  
 torus types are metallic.

K.R. Dienes and T. Brooks-Thomas,  
 ArXive: cond-mat.mes-hall/1005.4413v2.



$\tau_1$	$\tau_2$	$\tan \beta$	metal?	sample ( $m, n, p, q$ )
0	$\sqrt{3}$	0	yes	(12, 15, 42, 51)
0	$3\sqrt{3}$	$\sqrt{3}/3$	yes	(10, 13, -34, -46)
0	$9\sqrt{3}$	0	no	(10, 8, -39, -33)
0	$9\sqrt{3}$	$\sqrt{3}/27$	no	(19, 17, -66, -60)
1/3	$\sqrt{3}$	0	no	(10, -6, -33, 18)
-1/3	$\sqrt{3}$	0	no	(10, -4, 33, -15)
1/4	$3\sqrt{3}/4$	$\sqrt{3}/3$	yes	(10, 16, -32, -53)
-1/4	$3\sqrt{3}/4$	$\sqrt{3}/3$	yes	(10, 1, -32, -5)
1/4	$9\sqrt{3}/4$	0	no	(10, -1, 32, -5)
-1/4	$9\sqrt{3}/4$	0	no	(10, 18, -34, -63)
3/7	$9\sqrt{3}/7$	$\sqrt{3}/2$	no	(10, 14, 32, 43)
-3/7	$9\sqrt{3}/7$	$\sqrt{3}/5$	no	(10, 12, 34, 39)
2/13	$9\sqrt{3}/13$	$\sqrt{3}/7$	no	(10, 11, -32, -37)
-2/13	$9\sqrt{3}/13$	$3\sqrt{3}/5$	no	(10, 14, -33, -48)



## **NSF XSEDE (formerly TeraGrid) – Petascale Computing**

*2011 UPEP Project with summer student Adam Byrd:*

C++ codes with MPI parallelism for large-scale parallel simulations of ring currents (> 20,000 atoms, different chiralities).

Realistic carbon nanoring diameters  $d = 200 - 500 \text{ nm}$ .

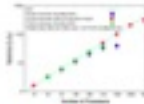
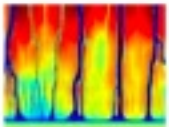
Use of linear libraries (**PETSC**) for Hamiltonian matrix inversion (dense/sparse); 64 – 1024 processors.

Resources: TACC ‘Ranger’ (XSEDE); FSU HPC; U Miami ‘Pegasus’.

**GOAL:**      ***I-V curve for one B-field value in a few mins/hours.***  
                 **→ magnetoresistance I-B, multipole radiation, ...**

# PETSc

- Home



## Portable, Extensible Toolkit for Scientific Computation

- [Download](#)

The current version of PETSc is [3.2](#); released [Sept 8, 2011](#).

- [Features](#)

- [Documentation](#)

- [Manual pages and Users Manual](#)

- [Referencing PETSc](#)

- [Tutorials](#)

- [Installation](#)

- [Logs](#)

- [AMS](#)

- [Changes](#)

- [BugReporting](#)

- [CodeManagement](#)

- [FAQ](#)

- [License](#)

- [Applications/Publications](#)

- [Miscellaneous](#)

- [External Software](#)

- [Developers Site](#)

PETSc, pronounced PET-see (the S is silent), is a suite of data structures and routines for the scalable (parallel) solution of scientific applications modeled by partial differential equations. It employs the [MPI standard](#) for parallelism.

- [Scientific applications](#) that use PETSc

- [Features](#) of the PETSc libraries (and a recent [podcast](#))

- [Linear system solvers](#) accessible from PETSc

- Related packages that use PETSc

- [TAO - Toolkit for Advanced Optimization](#)

- [SLEPc - Scalable Library for Eigenvalue Problems](#)

- [Fluidity - a finite element/volume fluids code](#)

- [Prometheus - scalable unstructured finite element solver](#)

- [freeCFD - general purpose CFD solver](#)

- [OpenPVM - finite volume based CFD solver](#)

- [OOFEM - object oriented finite element library](#)

- [libMesh - adaptive finite element library](#)

- [DEAL\\_II - sophisticated C++ based finite element simulation package](#)

- [Python Bindings](#)

- [petc4py](#) from Lisandro Dalcin at CIMEC

- [Elefant](#) from the SML group at NICTA

- [Packages](#) that PETSc can optionally use

- PETSc is part of the [DOE SciDAC TOPS](#) project in algorithms, software, and applications for the scalable solution of PDEs.

PETSc is developed as [open-source](#), requests and [contributions](#) are welcome.

---

[Who are we?](#)

[Mailing Lists](#)

[Questions and Bug Reports](#)

[Referencing PETSc](#)

[Applications](#)

[Acknowledgements](#)

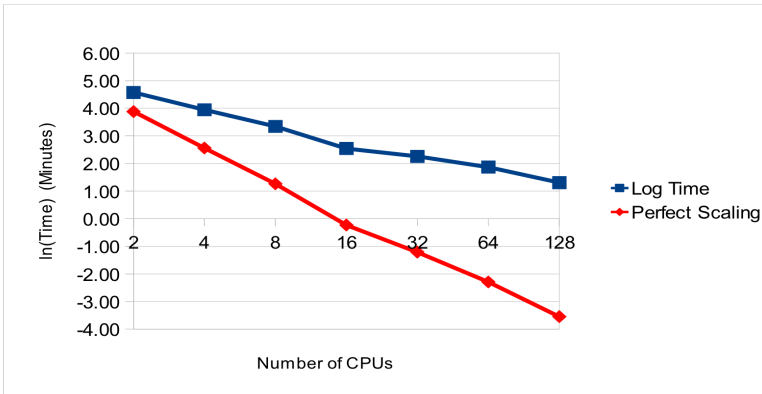
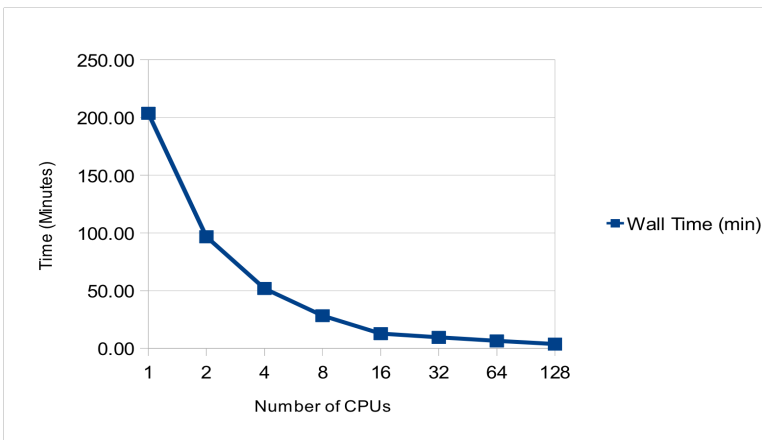
[FAQ](#)

[Tutorials](#)

[Funding](#)

## Benchmarking and scaling behavior for XRAC / XSEDE

Cntr Run Times						
CPUs	Log Time	Wall Time (min)	Wall Time (s)	CPU Time	Reported Time	Perfect Scaling
1	5.32	203.50	12210.00	12210	03:23:58	5.32
2	4.57	96.70	5802.00	11604	01:36:47	3.88
4	3.95	51.75	3105.25	12421	00:51:47	2.56
8	3.34	28.29	1697.50	13580	00:29:10	1.26
16	2.54	12.71	762.75	12204	00:12:44	-0.23
32	2.26	9.54	572.22	18311	00:09:42	-1.21
64	1.87	6.48	388.72	24878	00:06:45	-2.29
128	1.31	3.69	221.52	28355	00:03:55	-3.55





## ***QM corrections – Electron-phonon coupling***

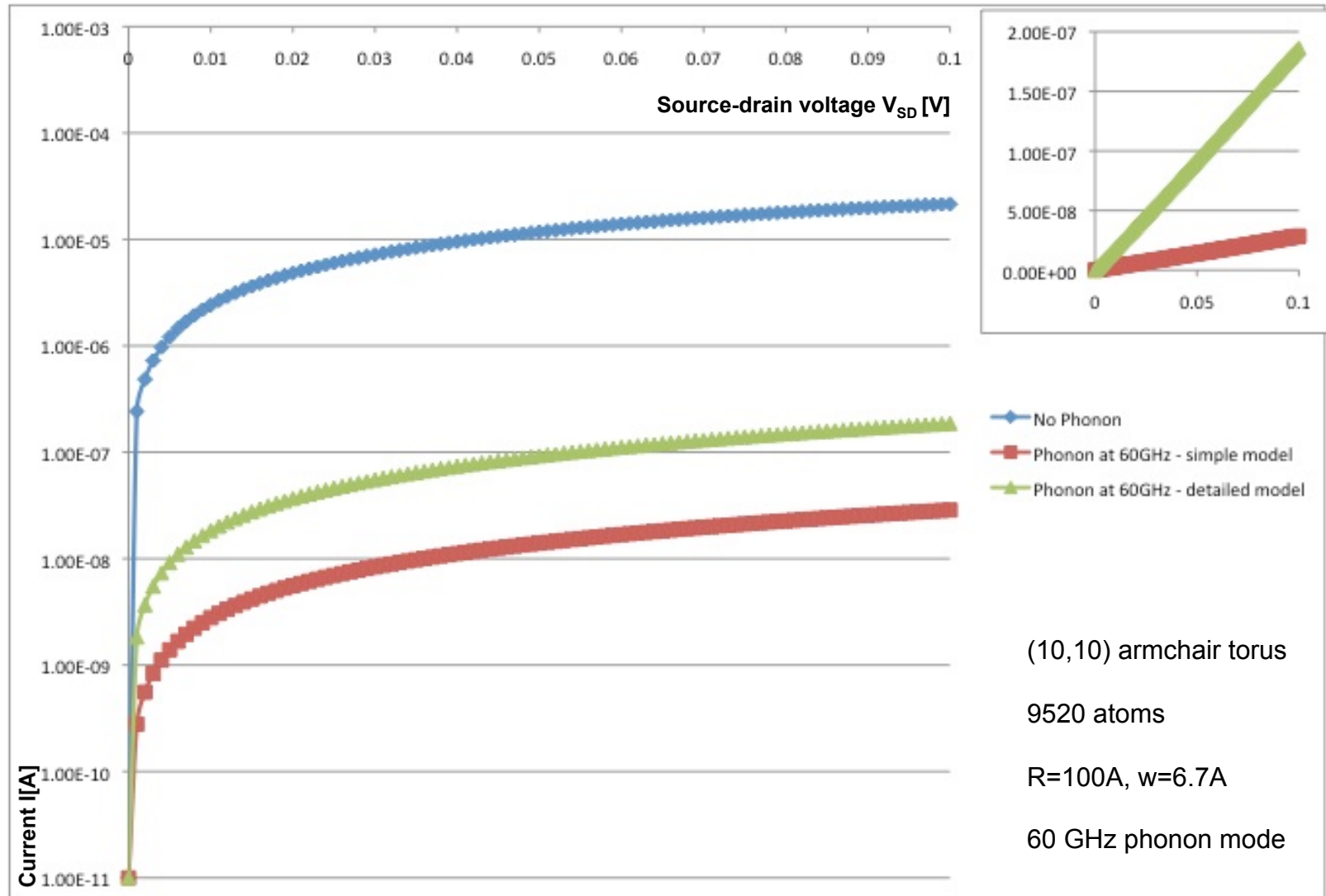
Collaboration with *Georgia Tech, Mechanical Engineering (M. Leamy)*:

Corrections to electron transport from *low-energy phonons* –

*Continuum model for long-wavelength phonons:*

- ✧ Continuum approximation for ring deformation due to atomic displacements in graphene lattice.
- ✧ Sheer/stress tensors, deformation potentials (finite-element code).
- ✧ Modified effective electronic hopping  $t_e$ , e-e-interaction, *electron-phonon coupling* in tightbinding transport calculation.

## *Quantum transport with electron-phonon coupling*



## ***FSU Shared-HPC Resources – code development & testing***

Number of Nodes:

404 Dell PowerEdge compute nodes

12 Dell PowerEdge login nodes

Storage:

156 TB (Panasas)

Number of Cores:

3,744 (+1584, Sep.'11 upgrade)

Further:

Several GPU devices (CUDA, openCL) and SMP machines (132 cores, 550 GB shared memory)

Memory: 8.2 TB

Network:

10 Gbps campus, 10 Gbps FLR connection



High Performance  
Computing @ FSU

A large, semi-transparent watermark graphic is centered over the server racks. It features the Florida State University logo at the top, which is circular with a stylized torch design and the text "FLORIDA STATE UNIVERSITY" around the perimeter. Below the logo, the words "High Performance Computing @ FSU" are written in a large, serif font.

## **TACC Sun Constellation Linux Cluster: ‘Ranger’ – production runs**

System Name: Ranger

Operating System: Linux

Number of Nodes:  
3,936

Number of Processing Cores:  
62,976

Total Memory:  
123 TB

Peak Performance:  
579.4 TFlops

Total Disk:  
1.73 PB (shared)  
31.4 TB (local)



<http://www.tacc.utexas.edu/resources/hpc>



# *Hubbard model for exciton generation and transport*

## *Hamiltonian:*

$$H = \sum_{i,j}^N \left( T_e c_i^\dagger c_j + T_h d_i^\dagger d_j \right) + h.c. + \sum_i^N U c_i^\dagger c_i d_i^\dagger d_i + \sum_{i \neq j}^N U_{NN} c_i^\dagger c_i d_j^\dagger d_j$$

$c_i^\dagger, c_j$  ( $d_i^\dagger, d_j$ )    electron (hole) creation / annihilation operators

$$\sum_i^N U c_i^\dagger c_i d_i^\dagger d_i \quad \text{electron-hole interaction}$$

$$\sum_{i \neq j}^N U_{NN} c_i^\dagger c_i d_j^\dagger d_j \quad \text{long-range interaction}$$



## **Nanoplasmonics – exciton-plasmon coupling**

### *Plasmon:*

QM quasi-particle approximation for collective, coherent charge density fluctuations on a metallic surface or nanoparticle ( $E_p = 0.5 - 2 \text{ eV}$ ).

### *Exciton:*

Strongly bound electron-hole pairs on cnts / nanorings ( $E_b = 0.3 - 0.6 \text{ eV}$ ;  $E_g = 0 \dots 1 \text{ eV}$ ).

- Long-range Coulomb interaction between excitons mediated through plasmons (longitudinal/transversal).
- *Exciton-plasmon coupling* ( $E_{int} = 0.1 - 0.3 \text{ eV}$ ).
- New ‘exciton-plasmon’ quasi-particle description (resonance).



## **Hamiltonian with exciton-plasmon interaction**

Strong exciton-surface-plasmon coupling demonstrated for semiconducting and metallic carbon nanotubes.

*Hamiltonian:*  $H = H_{plasmon} + H_{exc} + H_{int}$

*Exciton-plasmon interaction:*

$$H_{int} = -\frac{e}{m_e c} \sum_{\bar{n}} \bar{A}(\bar{n}) \left[ \hat{p}_{\bar{n}} - \frac{e}{2c} \bar{A}(\bar{n}) \right] + \sum_{\bar{n}} \hat{d}_{\bar{n}} \nabla_{\bar{n}} \hat{\phi}(\bar{n})$$

*Bogoliubov canonical transformation ('diagonalization' - new quasi-particles):*

$$H_{int} = \sum_{\vec{k}, \mu=1,2} \hbar \omega_{\mu}(\vec{k}) \hat{\xi}_{\mu}^{\dagger}(\vec{k}) \hat{\xi}_{\mu}(\vec{k}) + E_0$$

I.V. Bondarev et al., Optics and Spectr. 108, 376 (2010), Phys. Rev. B80, 085407 (2009).  
V.N. Popov and L. Henrard, Phys. Rev. B70, 115407 (2004).



## **Metamaterial Simulations - *finite-difference time domain (FDTD)***

Optical transmission spectra and energy transport for a 2D/3D nanoring metamaterial via FDTD:

- ✓ Extract average response characteristics of individual nanoring under polarized electromagnetic illumination from quantum mechanics model (Hubbard model).
- ✓ Solve Maxwell equations for electromagnetic wave propagation in metamaterial.
- ✓ Examples for FDTD codes: *MIT Photonic Bands*; *MEEP (MIT)*; *lumerical (commercial)* ([http://www.nnin.org/nnin\\_compsim.html](http://www.nnin.org/nnin_compsim.html))

## Acknowledgments



*Mario Encinosa (collaborator) – Florida A&M University, Physics*

*Leon Durivage (summer student) – Winona State University (MN),  
BlueWaters Petascale Computing Summer Internship Program*

*Boyan Hristov (Ph.D. student) – Florida A&M University, Physics  
John Williamson (physics), Jeff Battaglia (physics), Harsh Jain (CIS)*

*Ray O’Neal – Florida A&M University, Physics*

*Tiki Suarez-Brown – Florida A&M University, SBI, Information Systems*

*Jim Wilgenbusch and FSU Department of Scientific Computing*

*Chris Hempel, Bob Garza – Texas Advanced Computing Center (TACC)*

*Scott Lathrop – NCSA, TeraGrid Pathways Program 2010*



# References

1. **MJ and M. Encinosa**, Quantum electron transport in toroidal carbon nanotubes with metallic leads. *J. Mol. Simul.* 34 (1), 9-16 (2008). ArXive: [quant-ph/0709.0760](https://arxiv.org/abs/quant-ph/0709.0760).
2. **M. Encinosa and MJ**, Dipole and solenoidal magnetic moments of electronic surface currents on toroidal nanostructures. *J. Computer-Aided Materials Design*, Vol. 14 (1), 65-71 (2007).
3. **M. Encinosa and MJ**, Excitation of surface dipole and solenoidal modes on toroidal structures (2006). ArXive: [physics/0604214](https://arxiv.org/abs/physics/0604214).
4. **M. Encinosa and MJ**, Elliptical tori in a constant magnetic field. *Phys. Scr.* 73, 439 – 442 (2006). ArXive: [quant-ph/0509172](https://arxiv.org/abs/quant-ph/0509172).
5. S. Iijima, Helical microtubules of graphitic carbon. *Nature (London)* 354, 56 (1991).
6. J.C. Charlier, X. Blase and S. Roche, Electronic and transport properties of carbon nanotubes, *Rev. Mod. Phys.* 79, 677 (2009).
7. A.H. Castro Neto et al., The electronic properties of graphene, *Rev. Mod. Phys.* 81, 109 (2009).
8. S. Datta, Electronic Transport in Mesoscopic Systems. *Cambridge Univ. Press* (1995).
9. M.P. Anantram and T.R. Govindan, *Phys. Rev. B* 58 (8), 4882 (1998).
10. T. Kaelberer et al., *Science* 330, pp. 1510 (2010).
11. S. Motavas, B. Omrane and C. Papadopoulos, *Langmuir* 25(8), pp. 4655 (2009).
12. M. Luisier and G. Klimeck, A multi-level parallel simulation approach to electron transport in nano-scale transistors. 2008 IEEE Proceedings. SC2008 November 2008, Austin, Texas, USA.
13. S. Balay et al., PETSc Web page, 2011. <http://www.mcs.anl.gov/petsc>
14. K.R. Dienes and T. Brooks-Thomas, Isospectral But Physically Distinct Modular Symmetries and their Implications for Carbon Nanotori. ArXive: [cond-mat.mes-hall/1005.4413v2](https://arxiv.org/abs/cond-mat.mes-hall/1005.4413v2) (Aug. 30, 2011).

